CrossMark

# Self-standing electrodes with core-shell structures for high-performance supercapacitors

Guanjie He[a], Min Ling[a], Xiaoyu Han[a], Dina Ibrahim Abou El Amaiem[b], Yuanlong Shao[c], Yaomin Li[a], Wenyao Li[d], Shan Ji[b], Bo Li[d], Yao Lu[a], Rujia Zou[d], Feng Ryan Wang[b], Dan J.L. Brett[b], Zheng Xiao Guo[a], Chris Blackman[a], Ivan P. Parkin[a],*

[a] *Christopher Ingold Laboratory, Department of Chemistry, University College London, 20 Gordon Street, London WC1H 0AJ, U.K.*
[b] *Electrochemical Innovation Lab, Department of Chemical Engineering, University College London, London WC1E 7JE, U.K.*
[c] *Cambridge Graphene Center, Department of Engineering, University of Cambridge, 9 JJ Thomson Avenue, Cambridge CB3 0FA, U.K.*
[d] *State Key Laboratory for Modification of Chemical Fibers and Polymer Materials, College of Materials Science and Engineering, Donghua University, Shanghai 201620, China*

## ARTICLE INFO

## ABSTRACT

Fabrication of supercapacitor devices with the carbon cloth supported $W_2N$@carbon ultrathin layer core-shell structures ($W_2N$@C CS/carbon cloth) were realized by aerosol-assisted chemical vapour deposition (AACVD) followed by an ammonia annealing process. The representative electrodes delivered excellent areal specific capacitance of 693.0 mF cm$^{-2}$ at 5 mV s$^{-1}$ in a three electrode testing system, good rate capability of ~ 78% retention when the scan rate increased 10 times and superior cycling stability with ~ 91% capacitance retention after 20,000 cycles. The self-standing electrodes were manufactured for flexible asymmetric supercapacitors and assembled into coin cells with ionic electrolyte for high working voltage applications. The primary origins for the outperformance of $W_2N$ over $WO_{3-x}$ in acid aqueous electrolytes are uncovered by electrochemical analysis, simulation work and *in-situ* transmission electron microscope (TEM). This discovery paved the way of exploring and designing advanced metal nitride electrode materials for supercapacitors.

## 1. Introduction

As promising energy storage devices, supercapacitors, in particular pseudocapacitors, can provide higher power densities than most of the batteries [1]. The practical applications of commonly reported pseudocapacitor electrodes, such as an amorphous structure based on $RuO_2$ [2,3], $MnO_2$ [4] and $WO_3$ [5], *etc.*, call for improvement on specific capacitance and energy density. Metal nitride, is a type of electrode materials that presents excellent electrical conductivity (4000–55500 S cm$^{-1}$) and will improve energy storage properties. Fan et al. fabricated asymmetric supercapacitors based on TiN cathodes and $Fe_2N$ anodes, leading to high rate and achieving stable energy storage devices [6]. They identified structural design modifications to solve the oxidation problem of metal nitrides, by methods such as carbon coating. Among all the reported metal oxides/nitrides materials in energy storage applications, tungsten-based electrodes have a series of inherent advantages, such as relatively low toxicity and cost, high theoretical specific capacitance and high stability [5,7,8]. There have been intensive studies focused on tungsten oxide materials to be

employed as pseudocapacitive electrodes: $MoO_{3-x}/WO_{3-x}$ core-shell nanowires [8]; nanoflower-like $WO_3$ on titanium foams [9] and $WO_3$/graphene composite aerogels [10]. These materials show improved electrochemical performances over pure $WO_3$ materials mainly through the nanostructure design. However, they still need further improvements, in fabrication techniques and performance amelioration to meet practical requirements. It is worth mentioning that there are few works that relate to tungsten nitride materials for energy storage applications [11] and no report has so far uncovered the origin of its high pseudocapacitive performance. In addition, no comprehensive research has been reported for the fabrication of devices based on tungsten nitride materials.

The methods for manufacturing self-standing electrodes involve integration of the active electrode materials and current collectors, such as elastic carbon films [12] and various metal substrates that support metal oxide materials [9,13], which avoids the complicated electrodes fabrication procedure for powdery materials. Compared with the most commonly reported self-standing electrode materials synthesis methods, such as the hydrothermal and electrochemical deposition

processes, chemical vapor deposition (CVD) has been demonstrated as an optimal method for surface engineering and provides promising advantages, such as being an industrially relevant technique for film production, production of uniform coatings [14]. Typically, CVD produces stronger adhesion strength between the active materials and the substrates. Recently, we have reported the growth mechanism of $WO_3$ nanorod arrays on glass by aerosol-assisted chemical vapour deposition (AACVD) method [14]. This method achieves films at relatively low coating temperature compared with other types of CVD [8,15] and is a potentially important technique for industrial applications due to the consequently reduced energy consumption.

The self-standing electrodes of core-shell structures on carbon cloth reported in this study were prepared by a single step AACVD ($WO_{3-x}$ formation and carbon coating in one step) followed by an ammonia annealing process. Vertically aligned nanorods on current collectors can significantly enhance the specific surface area and act as a matrix to support other metal oxides with low electrical conductivity, such as an amorphous structure of $RuO_x$ nanoparticles in this work. Supercapacitors were assembled by using a solid-state electrolyte for flexible devices and organic liquids for high voltage applications. The merits of enhanced electrochemical performances of $W_2N$ materials in aqueous acid electrolyte compared with oxide counterparts were unveiled by electrochemical performances testing, Density Functional Theory (DFT) calculations and *in-situ* transmission electron microscopy.

## 2. Results and discussion

The synthetic methodology for $W_2N@C$ core-shell arrays (CSA) involves two steps, as illustrated in Fig. 1. Firstly, $WO_{3-x}@C$ CSA nanostructures were directly grown onto substrates by using $[W(CO)_6]$ in a mixture of acetone and methanol as the precursor for both tungsten and carbon sources. The uniform coating on hard, soft and porous substrates (morphology characterization for $WO_{3-x}@C$ CSA on copper foils, nickel foams, carbon clothes in Figure S1) indicated that AACVD is a powerful technique for the fabrication of nanostructure film on various substrates. The mixture of acetone and methanol solution was used to accelerate the formation of aerosols during the AACVD process, thus decreasing the deposition temperature, making this method more suitable for commercialization (Figure S2 for installation of AACVD system). The second step is the annealing process of the $WO_{3-x}@C$ CS/carbon cloth in the tube furnace under a slow flow rate of ammonia gas at 600 ºC for 3 hours. The heating rate was controlled at 5 ºC/min for mild ion exchange chemical reactions without damaging the morphology of the nanorod arrays and the core-shell structures. With the phase change during the annealing process, the colour of the electrodes changed from blue to black.

The morphology of the carbon cloth supported $W_2N@C$ CSA was recorded by scanning electron microscopy (SEM) and shown in Fig. 2a. The $W_2N$ form as needle-like nanorod arrays. The uniform coating can be confirmed by the low-magnification SEM images. The detailed morphology of the $W_2N@C$ nanorod array clusters are revealed by

high-magnification SEM images in Fig. 2b. The width of the single nanorod is 20~30 nm and length is more than 1 μm. Fig. 2c shows transmission electron microscopy (TEM) image of a typical single $W_2N@C$ nanorod. The thin carbon shell can be detected to cover the $W_2N$ nanorod. The simultaneous $WO_{3-x}$ synthesis and carbon shell deposition during the AACVD process can be beneficial for stabilizing the metal nitrides and to further enhance the electrical conductivity. High resolution TEM (HRTEM) image were detected to reveal the clear nanostructure and phases, which displayed the carbon layer of ~ 3 nm as shown in Fig. 2d. The labelled lattice space of ~ 0.205 nm can be indexed to the (200) crystal plane of cubic structure of tungsten nitride. Those morphologies revealed by TEM images are similar to those of $WO_{3-x}@C$ nanorods (Figure S3a, b), indicating the ammonia annealing process had no influence on the morphology of the nanorod or the carbon shell. The blue dashed circle showed the typical amorphous carbon lattice. To further illustrate the structure of the carbon cloth supported $W_2N@C$ CS nanorods, scanning electron microscopy-energy dispersive X-ray spectroscopy (SEM-EDS) characterization was performed to obtain elemental composition and distribution information. EDS spectra revealed the target element peaks of C, W, N in the whole of the nanostructures. Fig. 2(g-i) showed the SEM mapping images of the $W_2N@C$ CS/carbon cloth. The dense red spots proved the high tungsten content. Nitrogen overlapped with tungsten homogeneously, demonstrating nitrogen was uniformly distributed in the crystal structures. Moreover, the carbon was present at low density, corresponding to the thin layers detected from the TEM images.

X-ray Diffraction (XRD) patterns were recorded to investigate the phase changes of the electrodes before and after the annealing process in ammonia gas. The phase of the $WO_{3-x}$ (Figure S3c) can be indexed to $W_{18}O_{49}$ (JC-PDS No. 36–0101) and $W_5O_{14}$ (JC-PDS No. 41–0745) while the blue color of the coating indicated the oxygen vacancy features of the tungsten oxide. After the reaction with the ammonia, it is clearly observed that pure phase of $W_2N$ was achieved successfully and the diffraction peaks of ~ 17.1º, ~ 19.8º, ~ 28.1º, ~ 33.1º and ~ 34.6º correspond to the cubic $W_2N$ lattice of (111), (200), (220), (311) and (222) (JC-PDS No. 25–1257) with no XRD evidence of the oxide phase in Fig. 3a. The carbon peak at ~ 12º from the carbon ultrathin shell/carbon cloth substrates can be detected from both the XRD patterns before and after the annealing process in the ammonia gas. X-ray photoelectron spectroscopy (XPS) analysis showed that the C-N bonds present from C 1 s (Fig. 3b) and N 1 s (Fig. 3d) spectra, indicating the N doping into the carbon frameworks with $sp^3$ and $sp^2$ hybridized orbitals [16]. Compared with $WO_{3-x}$ in Figure S3d, the W 4 f spectrum of $W_2N$ (Fig. 3c) showed different compositions, which was in accordance with the Raman spectra results (Figure S4). The spin orbital positions of the W $4f_{7/2}$ and W $4f_{5/2}$ electron for W at ~ 33.2 and ~ 35.2 eV are related to W within the b.c.c $W_2N$ structures. The chemical shifts in the core levels of the $W_2N$ relative to W compared with the results from the literature which correspond to a charge transfer from tungsten to nitrogen during the ammonification process [17]. The W 4 f spectrum of $W_2N$ has some residual W-O bond as $WO_{3-x}$, which was caused by a surface oxygen contamination layer, which is a
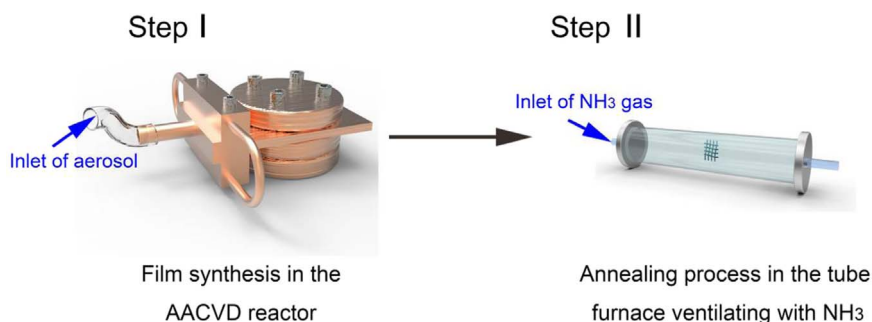


**Fig. 1.** Schematic illustration of the synthetic procedure of the electrodes. Two step synthesis of the carbon cloth supported $W_2N@C$ core-shell arrays (CSA) electrodes.